Ionics (2019) 25:241–251
https://doi.org/10.1007/s11581-018-2582-7

ORIGINAL PAPER

A new solid-state electrolyte based on polymeric ionic liquid for high-performance supercapacitor

Xinge Wen[1] · Tao Dong[2] · Ao Liu[2] · Shuohang Zheng[2] · Shimou Chen[2] · Yifan Han[1] · Suojiang Zhang[2]

Received: 19 March 2018 / Revised: 23 April 2018 / Accepted: 26 April 2018 / Published online: 21 May 2018

Abstract

As a polymer host, one polymeric ionic liquid poly(methyl methacrylate-1-vinyl-3-ethyl-imidazolium bis(trifluoromethylsulfonyl) imide) (abbr. P(MMA-co-VEImTFSI)) was successfully synthesized and characterized. Four poly(vinylidene fluoride-co-hexafluoropropylene) (abbr. PVDF-HFP)-based polymer electrolytes were prepared by blending 0, 5,15, and 25 wt% P(MMA-co-VEImTFSI). The electrochemical performances of the prepared electrolytes were studied carefully. The results revealed that increasing the polymeric ionic liquid content, the ionic conductivity of the polymer electrolytes could be enhanced and it obeyed the Arrhenius rule. The highest ionic conductivity of the polymer electrolytes was up to 2.09×10^{-3} S cm^{-1} at room temperature. The polymer with 25 wt% polymeric ionic liquid showed an excellent electrochemical performance for supercapacitor electrolyte. After 2000 cycles, the retention of capacitance in P(MMA-co-VEImTFSI)-based polymer electrolyte was above 80%. It implied that the present P(MMA-co-VEImTFSI) polymeric ionic liquid was a decent component candidate in the high-performance polymer electrolytes.

Keywords Polymeric ionic liquid · Solid-state electrolyte · Supercapacitor · High conductivity

Introduction

With the fast growth demand of high-performance energy storage systems for practical application in electronics, wearable devices, and medical instruments technology, the batteries which are lighter, safer, and more flexible are growing significantly [1, 2]. The conventional lithium-ion batteries and supercapacitors with liquid electrolytes exhibit excellent electrochemical performances, but the drawbacks of fire, leakages, and explosions cannot be neglected [3, 4]. Many considerable efforts have been devoted to the solid electrolyte such as polymer electrolytes and inorganic solid electrolytes [5–7]. Polymer electrolyte with the outstanding advantages of flexibility, no leakages, safety, and environmental friendliness has attracted much attention, which can be easy to design the shape, and tune the properties by choosing different polymers [8–11]. Various polymer electrolytes are consisted of poly(ethylene oxide) (PEO), poly(vinylidene fluoride-co-hexafluoropropylene) (PVDF-HFP), or poly(methyl methacrylate) (PMMA) as polymer matrix. However, the polymer electrolytes have low ionic conductivity between 10^{-8} and 10^{-7} S cm^{-1} due to the high crystalline of the polymer matrix, which inhibit their practical application [12, 13]. As of now, many efforts have been made to enhance the ionic conductivity such as forming plasticizers, adding ionic liquids, dispersing inorganic nanoparticles, and blending different polymers [14–17].

Polymeric ionic liquids (PILs) are kinds of ionic conductive compounds containing ionic liquids (ILs) species in monomer repeating units, which retain the special properties both of ILs and of polymers [18–20]. Recently, PILs have attracted great attention as excellent candidates for polymer electrolytes because of their high thermal stability, good film-forming ability, and chemical compatibility [21–25]. Marcilla et al. reported ternary polymer electrolytes containing the pyrrolidinium-based polymeric ionic

✉ Yifan Han
yifanhan@ecust.edu.cn

✉ Suojiang Zhang
sjzhang@ipe.ac.cn

[1] School of Chemical Engineering and Energy, Zhengzhou University, Zhengzhou 450001, China

[2] Beijing Key Laboratory of Ionic Liquids Clean Process, State Key Laboratory of Multiphase Complex Systems, CAS Key Laboratory of Green Process and Engineering, Institute of Process Engineering, Chinese Academy of Sciences, Beijing 100190, China

liquids for lithium batteries exhibiting acceptable conductivity, time-stable interfacial resistance values, and good lithium stripping/plating performance [26]. Yang and coworkers have made a lot of work in terms of the polymer electrolytes containing PILs [27–33]. They synthesized PIL based on guanidinium cations and the dicationic polymeric ionic liquid poly[VIm][TMEN][TFSI] as polymer hosts, which effectively improved the rate performance for Li/$LiFePO_4$ cells at 25 and 80 °C, respectively.

Moreover, the abovementioned electrolytes have been successfully applied in lithium ion batteries; the supercapacitors with polymer electrolyte based on PIL did not show excellent electrochemical performance. Marcilla et al. reported polymer electrolyte consisting of a binary blend of a pyrrolidinium-based polymeric ionic liquid and pDADMATFSI [34]. The specific capacitance and real energy of supercapacitor were slightly lower than those obtained for convectional supercapacitors using pure PYR_{14}TFSI. In this work, a imidazolium-based polymeric ionic liquid poly(methyl methacrylate-1-vinyl-3-ethyl-imidazolium bis(trifluoromethylsulfonyl) imide) was synthesized and used as a solid polymer host to improve the electrochemical performance for supercapacitor. A comparative study for polymer electrolytes with different contents of PIL was carried out to identify the role of the PIL.

Experimental

Materials

The poly(vinylidene fluoride-co-hexafluoropropylene) (PVDF-HFP, Mw~455,000) was purchased from Sigma-Aldrich and used without further purification. The 1-ethyl-3-methylimidazolium bis(trifluoromethylsulfonyl) imide ([Emim][TFSI]) was purchased from Linzhou keneng cailiao Technology Co., Ltd. The 1-vinylimidazole (VIm ≥ 99%, Aladdin), 2,2′-azobis(2-methylpropionitrile) (AIBN, 99%, Aladdin), bromoethane (≥ 99%, Aladdin), and methyl methacrylate (MMA, ≥ 99%, Aladdin) were recrystallized and distillated before using. All the other regents were analytical grade.

Synthesis of polymeric ionic liquid and blend polymer electrolyte based on P(MMA-co-VEIm-TFSI)/PVDF-HFP

Synthesis of polymeric ionic liquid P(MMA-co-VEIm-TFSI)

The P(MMA-co-VEIm-Br**)** was prepared by the modified literature method [35], which is shown in Scheme 1. Firstly, the radical polymerization process was taken. A certain molar ratio of MMA was added to the 1-vinylimidazole (VIm) in acetonitrile solution using AIBN as the initiator at 65 °C for 48 h with the efficient stirring under nitrogen atmosphere. The raw product was obtained by precipitating the reaction mixture into deionized water, washing it for three times, and then drying it in a vacuum oven at 70 °C for 24 h. Secondly, the quaternization reaction between the above product and bromoethane was taken in methanol under nitrogen atmosphere at 40 °C for 24 h. The white solid product of P(MMA-co-VEIm-Br) was obtained after washing three times. Finally, the resulting P(MMA-co-VEIm-TFSI) was synthesized by anion exchange reaction of P(MMA-co-VEIm-Br) with LiTFSI for 24 h.

Preparation of blend polymer electrolyte based on P(MMA-co-VEIm-TFSI)/PVDF-HFP

The blend polymer electrolyte films P(MMA-co-VEIm-TFSI)/PVDF-HFP/[Emim][TFSI] were prepared as the following method: PVDF-HFP and appropriate quantities of P(MMA-co-VEIm-TFSI) (i.e., 0, 5, 15, and 25 wt%) were dissolved into the dimethylformamide (DMF) with vigorous magnetic stirring for 24 h to obtain a homogeneous solution. The required amount [Emim][TFSI] was added into the homogeneous polymer solution with stirring for 12 h. The blend polymer film was obtained by casting a well-homogenized slurry on a glass plate after evaporating the DMF slowly and cut into pellets. It was stored and handled inside an argon-filled glove box and maintained under argon atmosphere. The preparation process is presented in Scheme 1.

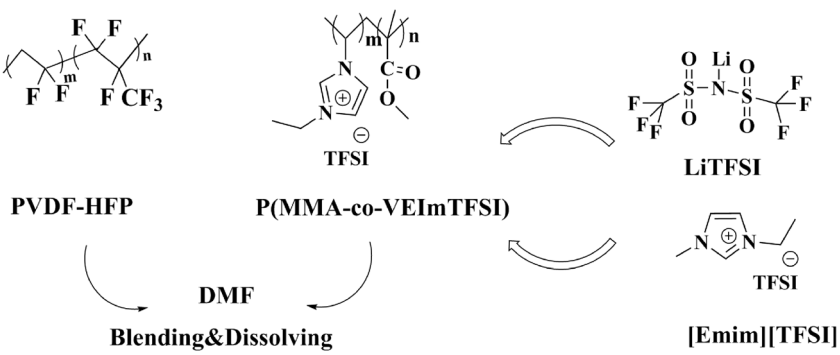

Scheme 1 The progress of preparation of polymer electrolytes with different contents of PIL

Characterization of polymeric ionic liquid and blend polymer electrolytes

Fourier transform infrared spectroscopy was characterized by an FTIR spectrometer (Nicolet 380, Thermo Electron). ^{1}H NMR spectroscopy of polymeric ionic liquid was taken on a 600-MHz NMR instrument (Avance III 600 MHz, Bruker) with deuterated chloroform as the solvent. The thermal stability of blend polymer electrolytes was performed on a thermogravimetric analyzer (DTG-60A, Shimadazu) from 30 to 600 °C at a heating rate of 10 °C min^{-1} under nitrogen atmosphere. The glass transition temperature of polymeric ionic liquid was measured by a DSC equipment (DSC 1, Mettler-Toledo) starting from − 80 to 250 °C at a heating rate 5 °C min^{-1} under nitrogen atmosphere.

The ionic conductivities of blend polymer electrolytes were measured using a symmetrical cell consisting of (the stainless steel) SS || blend polymer electrolyte || SS by an electrochemical workstation (CHI 660E, Shanghai Chenhua CH Instruments, Inc.) in the temperature range between 25 and 95 °C. The data was collected over a frequency range of 1 Hz–100 kHz with an amplitude of 5 mV at various temperatures. The ionic conductivities of the blend polymer electrolytes were calculated according to the following Eq. (1):

$$\sigma = \frac{L}{R \cdot S} \tag{1}$$

where L, R, and S represent the thickness, bulk resistance, and area of the polymer electrolytes, respectively.

The electrochemical stabilities of polymer electrolytes with different contents of polymerize ionic liquid were examined by linear sweep voltammetry (LSV) at a scan rate of 5 mV s^{-1} using (the stainless steel) SS || blend polymer electrolyte || SS cell from 0 to 6.0 V.

Electrochemical characterization of supercapacitors with blend polymer electrolytes

The symmetrical solid-state supercapacitor was assembled and gently pressed to evaluate the electrochemical properties of the polymer electrolyte with different contents of P(MMA-co-VEIm-TFSI). The cyclic voltammograms (CV) of the cell were performed in the potential range of 0 to 4.0 V at various scan rate. The charge-discharge measurements of the cells were conducted at 4.0 V with different current densities using the Land battery cycler (CT2001A, LAND Electronic Co. Ltd). The special capacitance, energy density, and power density of the cells were calculated according to the following Formulas (2), (3), and (4):

$$C_m = \frac{4I \times \Delta t}{m \times \Delta V} \tag{2}$$

$$E = \frac{C_m \times \Delta V^2}{2 \times 3.6} \tag{3}$$

$$P = \frac{E}{\Delta t} \times 3600 \tag{4}$$

where I is the discharge current (A), Δt is the discharge time (s), ΔV is the potential window during the discharge process after IR drop (V), and m is the total mass of the activated carbon on two electrodes (g).

Results and discussion

Characterizations of P(MMA-co-VEIm-TFSI)

The chemical structure of the PIL was confirmed by FTIR spectrum as shown in Fig. 1. The characteristic peaks at 3154 and 2952.48 cm^{-1} were attributed to the C–H stretching vibration in the imidazole ring and the saturated C–H stretching vibration of alkyl substituent on the imidazole ring, respectively. The characteristic peak at 1730.31 cm^{-1} was attributed to the –C=O stretching vibration of methyl methacrylate. The other characteristic peaks showed the skeletal vibration of imidazole ring at 1556.27 and 1449.28 cm^{-1}, and C–O–C stretching vibration at 1236.15 cm^{-1}. The results of the FTIR spectrum indicated that the structure of polymeric ionic liquid P(MMA-co-VEIm-TFSI) was synthesized successfully [35].

The ^{1}H NMR spectrum of polymeric ionic liquid P(MMA-co-VEIm-TFSI) using deuterated chloroform ($CDCl_3$) as solvent is shown in Fig. 2. It was noted that the chemical shifts appearing around 6.96–7.51 were attributed to the protons on the imidazole ring of N–CH=N and N–CH=CH–N,

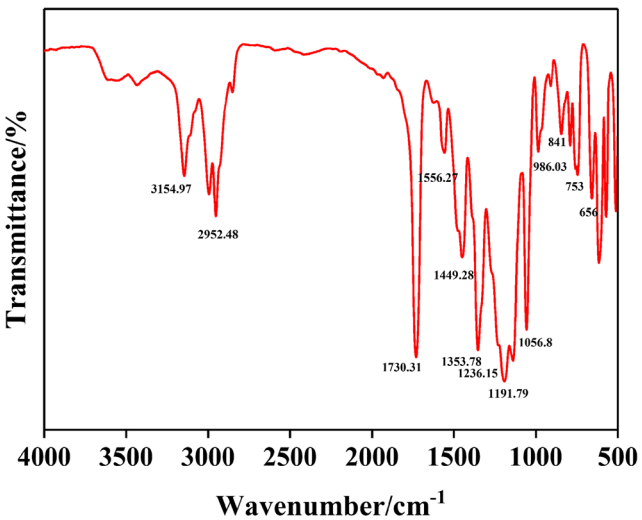

Fig. 1 The FTIR spectrum of P(MMA-co-VEIm-TFSI)

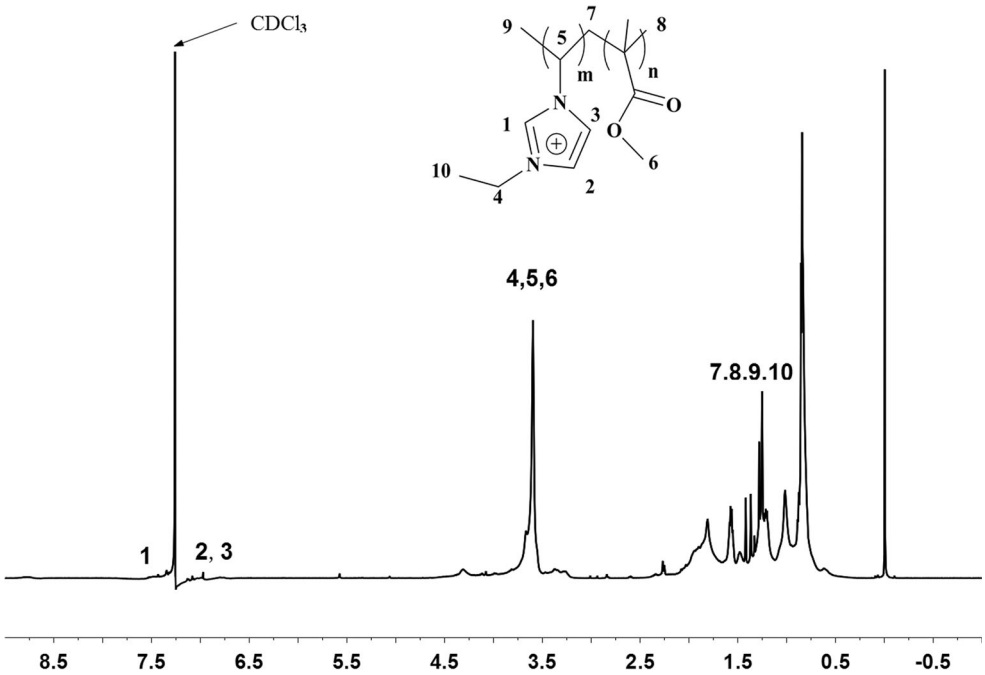

Fig. 2 The ^{1}H NMR spectrum of P(MMA-co-VEIm-TFSI) in $CDCl_3$

respectively. The chemical shifts of 4.31 and 0.89 were owing to the $–CH_2–CH_3$ of alkyl substituent on the imidazole ring. The other chemical shifts appearing at 3.60, 1.81, 1.02, and 0.84 were attributed to the protons on the ester, methyl, and methylene of P(MMA-co-VEIm-TFSI), respectively. All the chemical shifts were similar to the results of reference [36].

The molecular weight of polymer was an important character which was closely related to the conductivity behavior of the polymer electrolyte. Sekhon et al. reported that the conductivity of polymer electrolyte containing relatively low molecular weight of PMMA was higher than the corresponding liquid electrolytes [37]. The molecular weight of P(MMA-co-VEIm-TFSI) was investigated by GPC (*N*,*N*-dimethylformamide) and the result is shown in Fig. 3. The number average molar mass (M_n) and weight average molar mass (M_w) were about 3.23×10^4 and 3.41×10^4, respectively. The polydispersity (M_z/M_w) of the P(MMA-co-VEIm-TFSI) was 1.05.

The DSC curves of P(MMA-co-VEIM-TFSI) and PVDF-HFP were recorded in Fig. 4. Compared with the PVDF-HFP, the single glass transition temperature (Tg) of P(MMA-co-VEIM-TFSI) was occurred at around 113.04 °C, which indicated that it is an amorphous polymer. As far as we know, the polymers with lower melting point had higher conductivities [38, 39]. The result of DSC illustrated that P(MMA-co-VEIM-TFSI) used as the polymer host could improve the conductivity of polymer electrolyte.

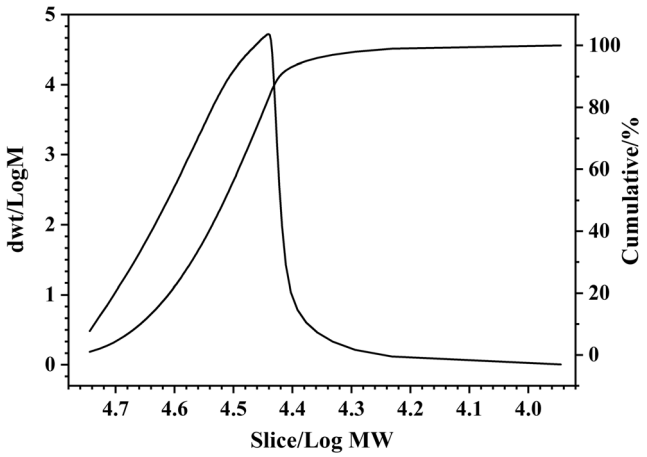

Fig. 3 The GPC chromatography of P(MMA-co-VEIm-TFSI) in DMF

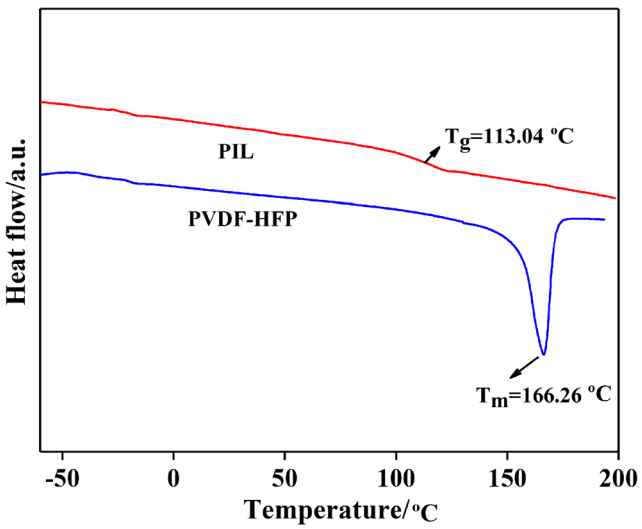

Fig. 4 The DSC of P(MMA-co-VEIm-TFSI) and PVDF-HFP

Properties of blend polymer electrolytes

The curves of the blending polymer electrolytes with different contents of polymeric ionic liquid are presented in Fig. 5. From Fig. 5a, the thermal decomposition of the four polymer electrolytes occurred in one distinct step, which showed almost no weight loss up to 275 °C. The total weight loss from 275 to 375 °C was possibly associated with the loss of ionic liquid and polymer backbone [40, 41]. The TGA results indicated that all the electrolytes displayed excellent thermal stabilities. Furthermore, the thermal shrinkage performances of the four polymer electrolytes were tested by resting them at 150 °C for 4 h as shown in Fig. 5b. It was obvious that the shape and size with the adding of 25 wt% P(MMA-co-VEIm-TFSI) had almost no change, which is an important character for using it as electrolyte/separator component.

The ionic conductivity has been regarded as another crucial electrochemical property of polymer electrolyte. The Arrhenius plots of the conductivity of the polymer electrolyte with different contents of P(MMA-co-VEIm-TFSI) are displayed in Fig. 6. Elevating temperature increased the electrolyte conductivity with growing tendencies for the four polymer electrolytes. The activation energy Ea of the four electrolytes was calculated according to the Arrhenius equation (Eq. 5) and the values were 0.3564, 0.3445, 0.2020, and 0.0705 eV. The lower activation energy was better for enhancing the ion migration [42].

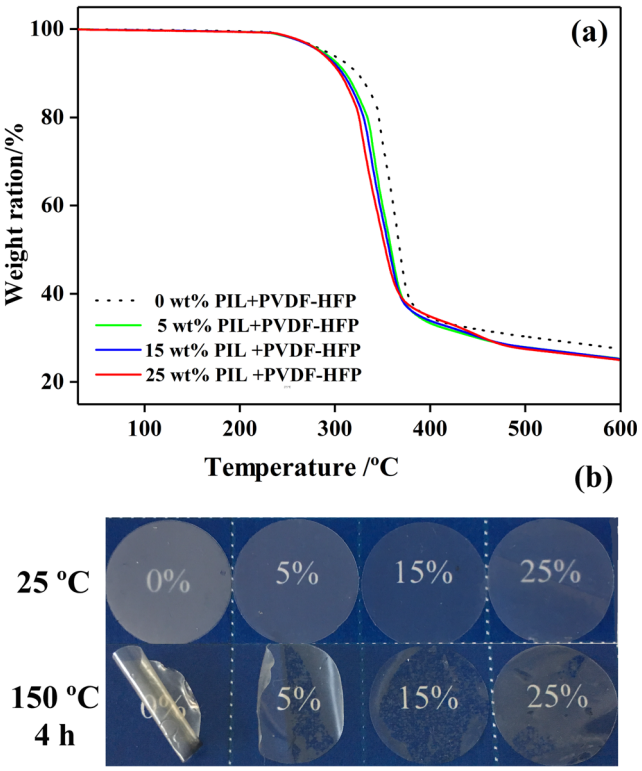

Fig. 5 **a** The TGA of polymer electrolytes with different contents of PIL. **b** The photograph of polymer electrolytes with different contents of PIL at 25 and 150 °C after 4 h

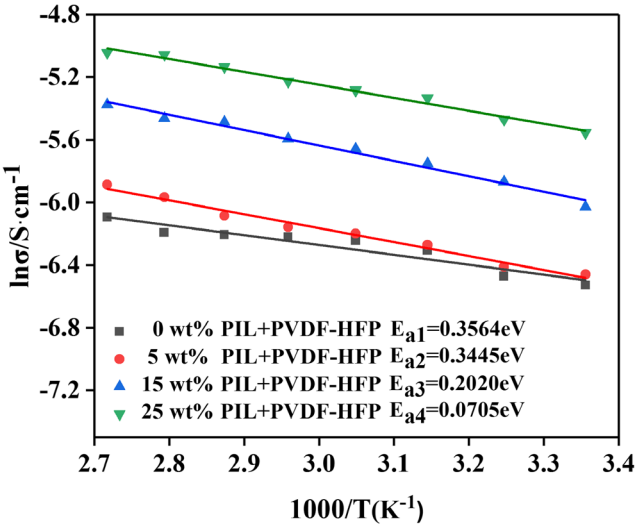

Fig. 6 The ionic conductivity of polymer electrolytes with different contents of PIL

$$\ln\sigma = \ln A + \frac{Ea}{RT} \tag{5}$$

The conductivities of the polymer electrolyte increased with the increasing content of PIL and reached a maximum value of 2.09×10^{-3} S cm^{-1} with the addition of 25 wt% PIL. It was sticky and it was hard to form the membrane when the addition of PIL was increased over 30%. Compared with the polymer electrolyte with the addition of 0 wt% PIL, the ionic conductivity was increased by 20%. This may be due to the amorphous region of the adding PIL which can affect the ionic conductivity by weakening the resistance above the segmental motion of the polymer chains [43].

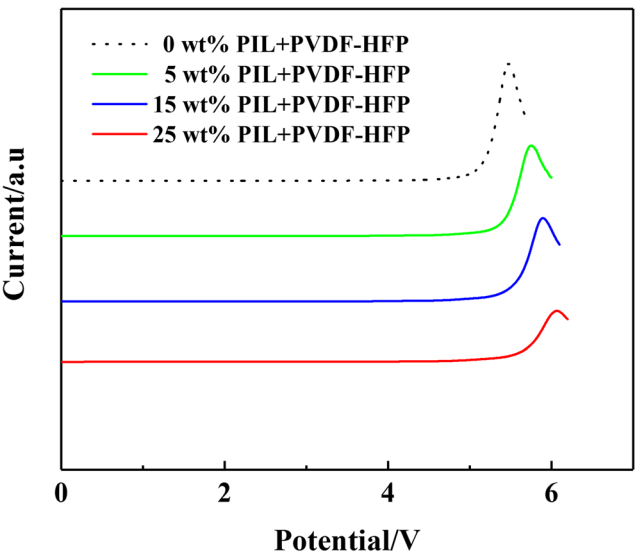

Fig. 7 The linear sweep voltammogram of polymer electrolytes with different contents of PIL at 5 mV s^{-1}

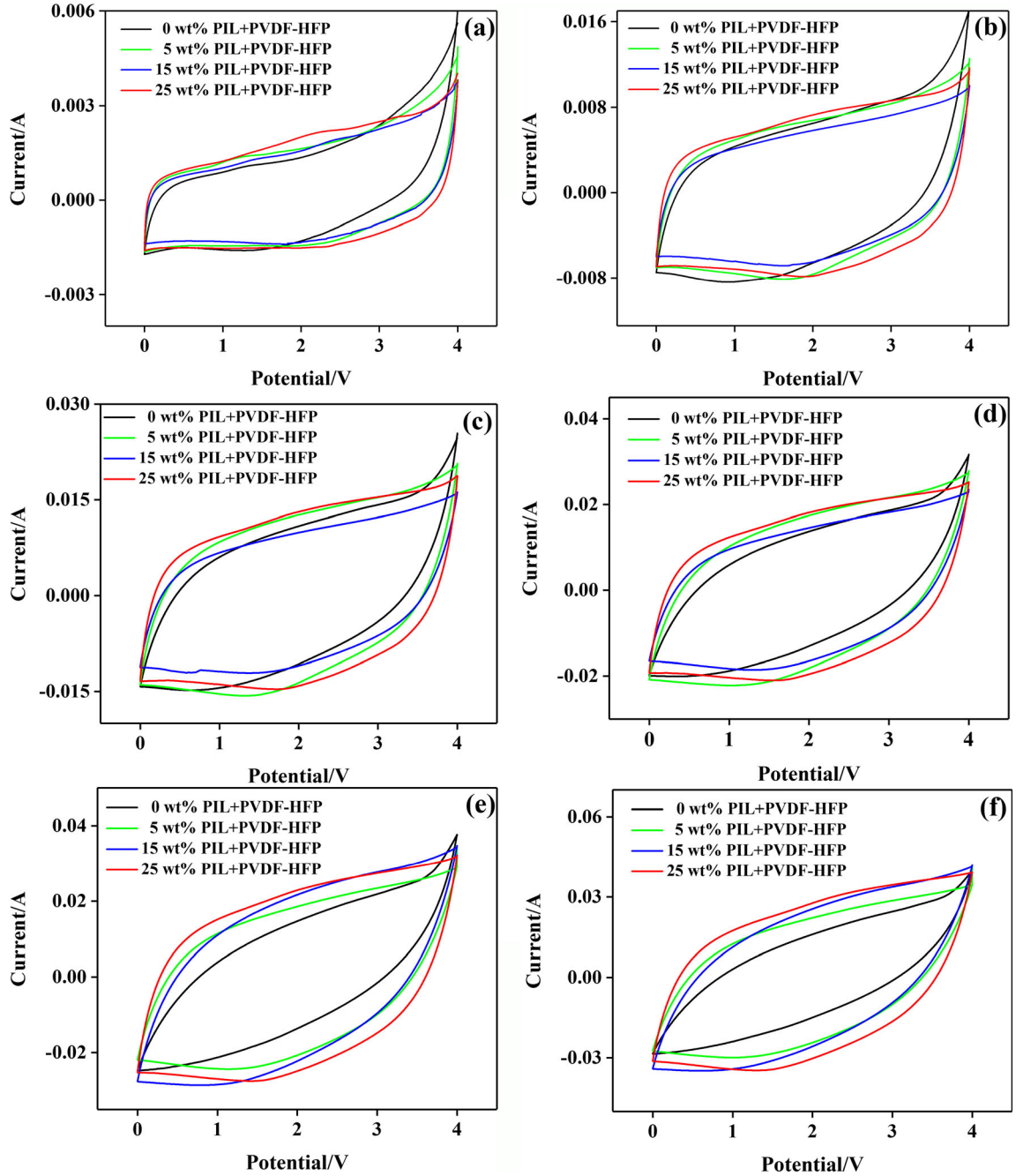

Fig. 8 The cycle voltammogram of polymer electrolytes with different contents of PIL at different rates. **a** 10 mV s^{-1}. **b** 50 mV s^{-1}. **c** 100 mV s^{-1}. **d** 150 mV s^{-1}. **e** 200 mV s^{-1}. **f** 250 mV s^{-1}

The LSV curves of the polymer electrolytes with different contents of PIL are depicted in Fig. 7. It was noted that all the polymer electrolytes can be stabilized at the voltage range between 0 and 5.6 V. The electrochemical window of polymer electrolytes was wider with the increasing content of PIL; when the content is 25 wt%, the value can reach to 5.53 V. This observation revealed that PIL blending can improve the electrochemical stability window of the polymer matrix. The result demonstrated that the blending electrolyte had good electrochemical stability; thus, it can be used as a candidate for good electrochemical energy storage devices.

Based on the above results, we can conclude that the polymeric ionic liquid P(MMA-co-VEIm-TFSI) is one of the effectively conductive polymer candidates as an additive in the polymer electrolyte due to its high conductivity, good thermal stability, and high electrochemical stability.

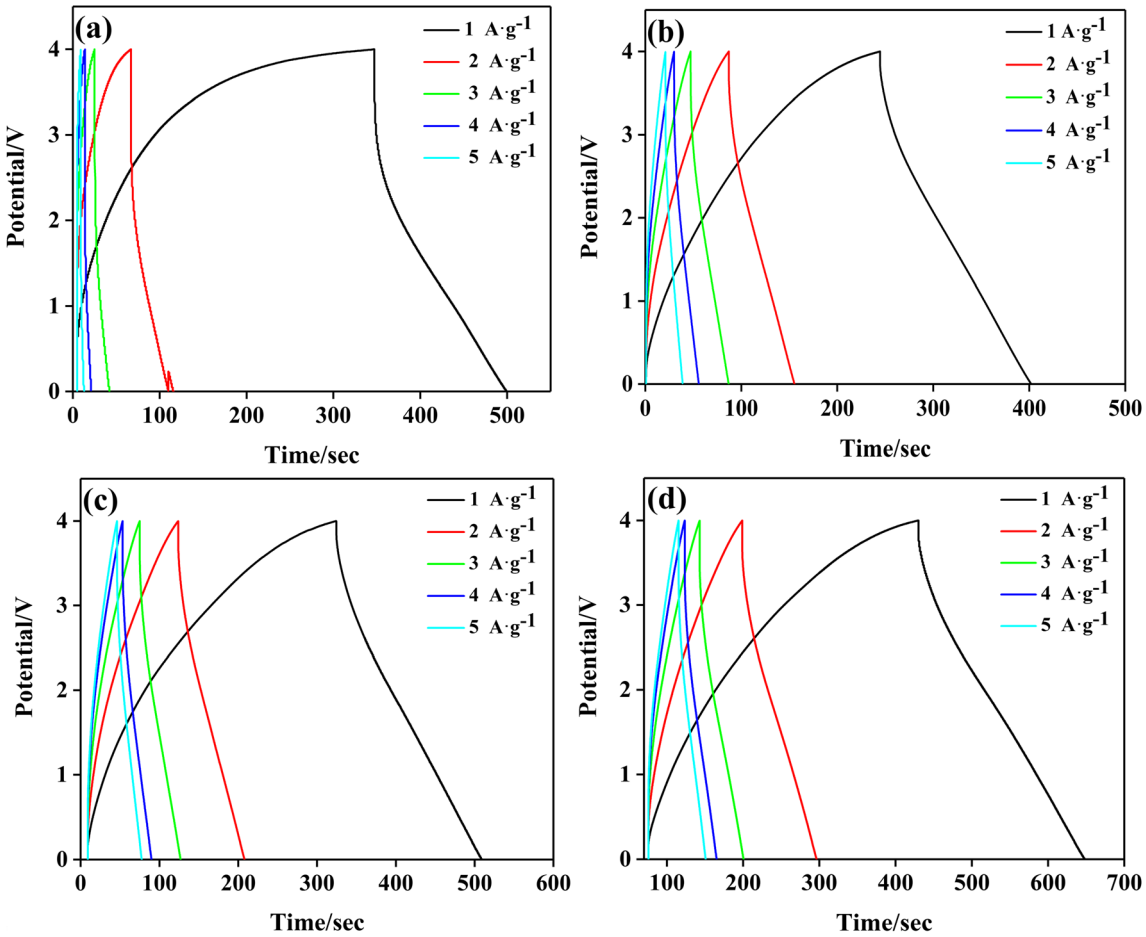

Fig. 9 The GCD curves of polymer electrolytes with different contents of PIL. **a** 0 wt% PIL. **b** 5 wt% PIL. **c** 15 wt% PIL. **d** 25 wt% PIL

Electrochemical performances of solid-state supercapacitor

To further verify the feasibility of the PIL-based polymer electrolyte applied in the practical energy storage systems, we designed a solid-state supercapacitor based on AC as the electrodes. The result of Fig. 8 showed that asymmetric CV profiles of the solid-state supercapacitor in the 0 to 4 V potential range at a variety of scan rates from 10 to 250 m·Vs^{-1}, stemming from the combination of fast electrolyte ion transport at the electrode. This phenomenon indicated a nearly rectangular shape response and little equivalent series resistance. Although

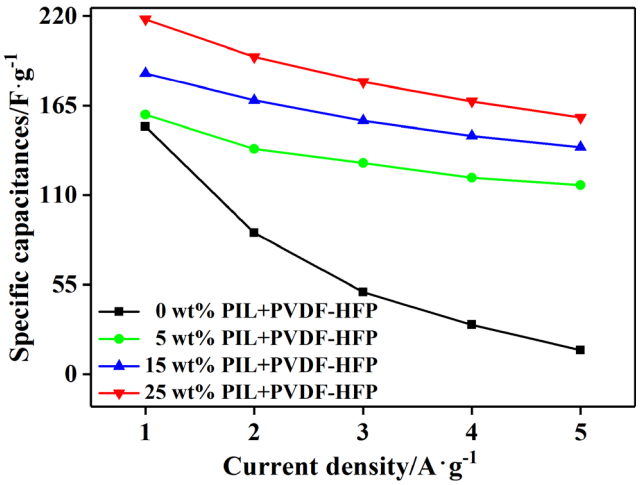

Fig. 10 The specific capacitances of polymer electrolytes with different contents of PIL under different current densities

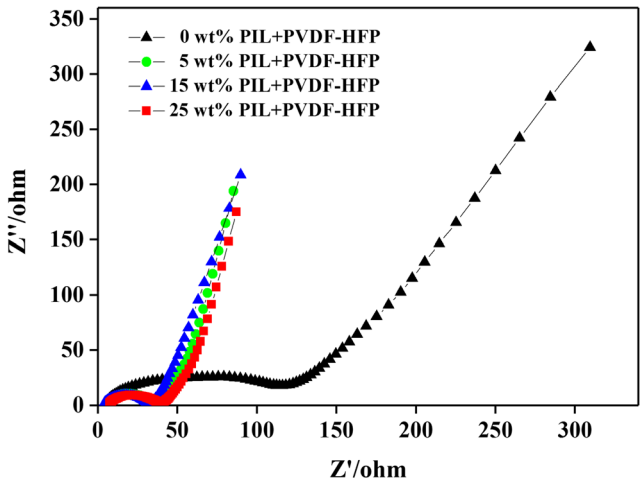

Fig. 11 The EIR of polymer electrolytes with different contents of PIL after 2000 cycles

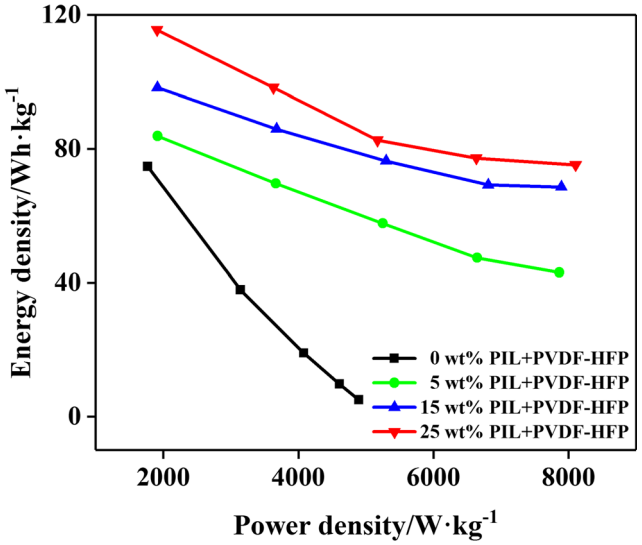

Fig. 12 The power density and energy of polymer electrolytes with different contents of PIL

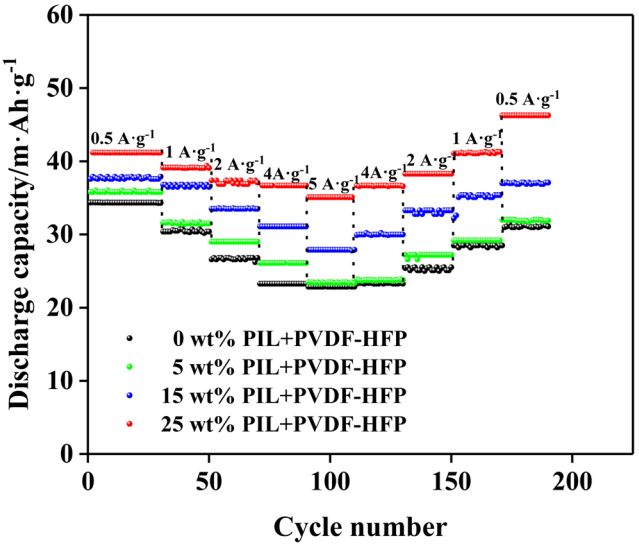

Fig. 14 The cycle curves of polymer electrolytes with different contents of PIL at different current densities

the shapes of the CV curves of polymer electrolytes with 0, 5, and 15 wt% PIL were similar to the electrolyte with 25 wt% PIL, the highest peak current of the electrolyte with 25 wt% PIL showed better charge transfer in the sample. Obviously, the integral area of the CV curve of the electrolyte with 25 wt% PIL was larger than the polymer electrolytes with 0, 5, and 15 wt% PIL, suggesting the highest electrochemical capacitance. Besides, the galvanostatic charge/discharge (GCD) curves displayed a symmetric quasi-triangular shape, which demonstrated the excellent combination of electrochemical performance [44]. Figure 9 exhibited the GCD curves of the solid-state supercapacitor with different mass ratios of PIL at the variety of current densities from 1 to 5 A g^{-1}. And the discharge time reaches a maximum value of 218 s when the current density is 1 A g^{-1}.

According to Eq. (2), the solid-state supercapacitor showed a specific capacitance of 219 F g^{-1} at 1 A g^{-1} (with respect to the mass of activated carbon) when using the 25 wt% PIL electrolyte (Fig. 10). At the high current density of 5 A g^{-1}, its specific capacitance of the supercapacitor with the polymer electrolyte adding 25 wt% PIL still remains 157 F g^{-1}.

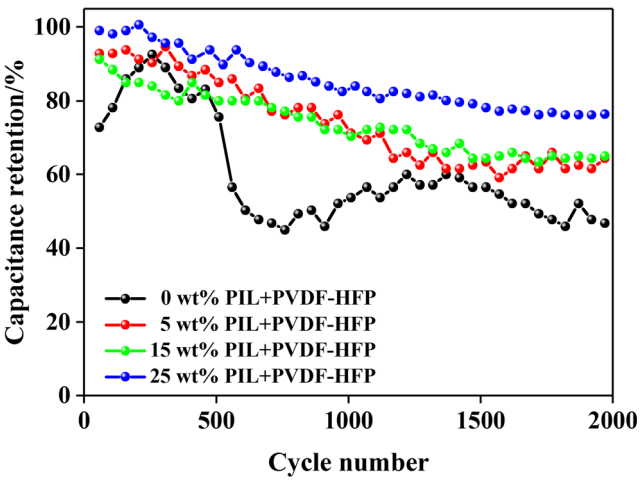

Fig. 13 The cycle curves of polymer electrolytes with different contents of PIL at 1 A g^{-1} current density

As shown in Fig. 11, the EIS curve was decreased with the increasing the amount of PIL added, which indicated the resistance was gradually smaller. These results suggested that the blending polymer electrolyte can improve the electrochemical performance of the supercapacitor. It can be attributed to the addition of PIL, which can increase the ionic conductivity of the electrolyte. The highly conductive property of the blending polymer electrodes was further proved by electrochemical series resistance, which demonstrated an extremely low resistance of 40 Ω with 25 wt% PIL blending polymer electrolytes.

The Ragone plots which showed the dependence of power density and energy density are illustrated in Fig. 12. Obviously, the energy density appeared decrement when power density increased. According to Eqs. (3) and (4), at room temperature, the maximum energy density of solid-state supercapacitors on the basis of the adding of 25 wt% PIL blending polymer electrolyte can approach 115.5 Wh kg^{-1} in a relatively low power density (1907.3 W kg^{-1}), and also it remained at 75.22 Wh kg^{-1} at a high power density (8104.5 W kg^{-1}); these values indicated the superior association of high energy and power density. The results showed that the adding of PIL devices achieved higher energy density than the other devices without PIL. To the best of our knowledge, this energy density was much better than the other different kinds of energy density (6.5 Wh kg^{-1}, 17.7 Wh kg^{-1}) previously reported [45–47].

The long cyclic durability was an important performance for electrochemical devices [48–50]. The cyclic stability of the polymer electrolyte with different contents of P(MMA-co-VEIm-TFSI) is displayed in Fig. 13. It can be found that the supercapacitor with the 25 wt% PIL had the highest

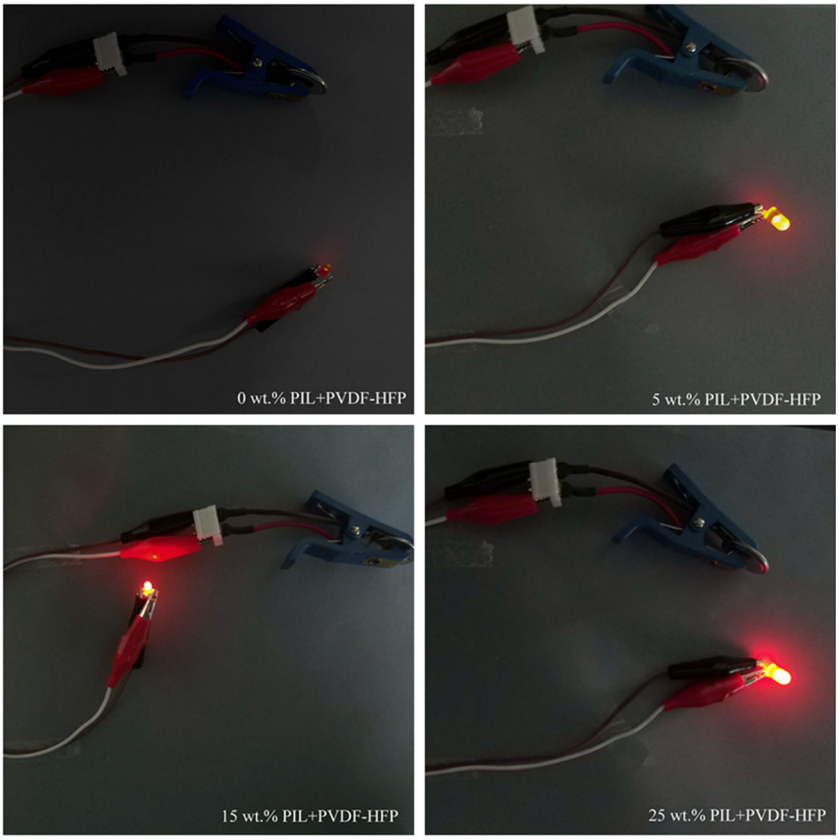

Fig. 15 The LED light of polymer electrolytes with different contents of PIL at the same condition

capacitance retention, which can be retained over 80% of the initial capacitance after 2000 charge-discharge cycles. However, it only retained 60% of the initial capacitance without PIL, indicating that the PIL can effectively improve the cyclic stability of the supercapacitor.

The long-term cyclic stability of the polymer electrolyte with P(MMA-co-VEIm-TFSI) demonstrated its implications for the high-performance supercapacitor. The rate capability data of the supercapacitor with/without PIL are presented in Fig. 14. The test consisted of a sequence of cycles performed successively at 0.5, 1.0, 2.0, 4.0, 5.0, 4.0, 2.0, 1.0, and 0.5 A g^{-1} for 20 cycles per current density. The supercapacitor with 0, 5, 15, and 25 wt% PIL delivered higher special capacitance under all different current densities. At 0.5 A g^{-1}, the special capacitance was 42, 38, 35, and 29 mAh g^{-1}, respectively. And the special capacitance of supercapacitor with 25 wt% PIL can reach 38 mAh g^{-1} up to 5.0 A g^{-1}, which was suggested that the PIL as the polymer host can efficiently enhance the conductivity of the polymer electrolyte.

A LED lighted by the commercial batteries (1.5 V pre-unit) to charge one device in series connection was also studied. The connected set could be fully charged within 2 s and light up a LED for several minutes. The supercapacitor energy storage devices with PIL made the LED let out a brighter light. The supercapacitor with 25 wt% PIL had the brightest light, demonstrating the high-efficient energy output ability of the devices and the good property of the PIL-based electrolyte, which coincided well with the abovementioned experimental results of conductivity, cyclic voltammetry, and cycling performance (Fig. 15).

Conclusions

The conductive polymeric ionic liquid P(MMA-co-VEIm-TFSI) was successfully prepared and used as the polymer host for the solid-state electrolyte. The polymer electrolyte with 25 wt% P(MMA-co-VEIm-TFSI) displayed a high ionic liquid of 2.09×10^{-3} S cm^{-1} at 25 °C and a broad electrochemical window of 5.0 V. When it was used in the supercapacitor, it also exhibited excellent electrochemical performance, with the capacitance, power density, and energy density as high as 219 F g^{-1}, 1907 W kg^{-1}, and 115.5 Wh kg^{-1} at the operating voltage of 4.0 V. Meanwhile, it can retain 80% capacitive retention after 2000 cycles. More importantly, the supercapacitor can drive the commercial LED light, and the supercapacitor with 25 wt% PIL had the brightest light, demonstrating the high-efficient energy output ability of the devices. Considering plenty amount of ionic liquids and their structure and function designable features, the electrolytes based on polymeric ionic liquids may pave a new way for constructing high-performance solid-state energy storage systems.

Funding information This work was supported financially by the National Key R&D Program of China (No. 2017YFB0102000), the National Natural Science Foundation of China (91534109, 51561145020), Key Research Program of Frontier Sciences, CAS(QYZDY-SSW-JSC011), CAS/SAFEA International Partnership Program for Creative Research Teams (20140491518), and Science and Technology Open Cooperation Project of Henan province (No. 17210110019).

References

1. Anothumakkool B, Torris ATA, Veeliyath S, Vijayakumar V, Badiger MV, Kurungot S (2016) High-performance flexible solid-state supercapacitor with an extended nanoregime interface through in situ polymer electrolyte generation. ACS Appl Mater Interfaces 8:1233–1241
2. Ahuja P, Sharma RK, Singh G (2015) Solid-state, high-performance supercapacitor using graphene nanoribbons embedded with zinc manganite. J Mater Chem A 3:4931–4937
3. Wang Q, Song WL, Fan LZ, Shi Q (2015) Effect of polyacrylonitrile on triethylene glycol diacetate-2-propenoic acid butyl ester gel polymer electrolytes with interpenetrating cross linked network for flexible lithium ion batteries. J Power Sources 295:139–148
4. Liu B, Huang Y, Cao HJ, Zhao L, Huang YX, Song AM, Lin YX, Li X, Wang MS (2017) A novel porous gel polymer electrolyte based on poly (acrylonitrile-polyhedral oligomeric silsesquioxane) with high performances for lithium-ion batteries. J Membr Sci 545:140–149
5. Wang YY, Hou BH, Guo JZ, Ning QL, Pang WL, Wang J, Lü CL, Wu XL (2018) An ultralong lifespan and low-temperature workable sodium-ion full battery for stationary energy storage. Adv Energy Mater 8:1703252
6. Guo JZ, Yang Y, Liu DS, Wu XL, Hou BH, Pang WL, Huang KC, Zhang JP, Su ZM (2018) A practicable Li/Na-ion hybrid full battery assembled by a high-voltage cathode and commercial graphite anode: superior energy storage performance and working mechanism. Adv Energy Mater 8:1702504
7. Hou BH, Wang YY, Guo JZ, Zhang Y, Ning QL, Yang Y, Li WH, Zhang JP, Wang X, Wu XL (2018) A scalable strategy to develop advanced anode for sodium-ion batteries: commercial Fe_3O_4 derived Fe_3O_4@ FeS with superior full-cell performance. ACS Appl Mater Interfaces 10:3581–3589
8. Pandey GP, Hashmi SA (2013) Ionic liquid 1-ethyl-3-methylimidazolium tetracyanoborate-based gel polymer electrolyte for electrochemical capacitors. J Mater Chem A 1:3372–3378
9. Bao JJ, Tao C, Yu R, Gao MH, Huang YP, Chen CH (2017) Solid polymer electrolyte based on waterborne polyurethane for all-solid-state lithium ion batteries. J Appl Polym Sci 134:45554
10. Gerbaldi C, Nair JR, Kulandainathan MA, Kumar RS, Ferrara C, Mustarelli P, Stephan AM (2014) Innovative high performing metal organic framework (MOF)-laden nanocomposite polymer electrolytes for all-solid-state lithium batteries. J Mater Chem A 2:9948–9954
11. Thayumanasundaram S, Rangasamy VS, Seo JW, Locquet JP (2015) Lithium polymer electrolytes based on sulfonated poly (ether ether ketone) for lithium polymer batteries. Eur J Inorg Chem 32:5395–5404
12. Li LB, Yang XY, Li JS, Xu YP (2018) A novel and shortcut method to prepare ionic liquid gel polymer electrolyte membranes for lithium-ion battery. Ionics 24:735–741
13. Liu LL, Li ZH, Xia QL, Xiao QZ, Lei GT, Zhou XD (2012) Electrochemical study of P(VDF-HFP)/PMMA blended polymer electrolyte with high-temperature stability for polymer lithium secondary batteries. Ionics 18:275–281
14. Dong Y, Ding TJ, Fan LZ (2017) A free-standing and thermostable polymer/plastic crystal electrolyte for all-solid-state lithium batteries. Ionics 23:3339–3345
15. Wang X, Yang CY, Wang GC (2016) Stretchable fluoroelastomer quasi-solid-state organic electrolyte for high-performance asymmetric flexible supercapacitors. J Mater Chem A 4:14839–14848
16. Huang Y, Zhong M, Shi F, Liu X, Tang Z, Wang Y, Huang Y, Hou H, Xie X, Zhi C (2017) An intrinsically stretchable and compressible supercapacitor containing a polyacrylamide hydrogel electrolyte. Angew Chem Int Ed 56:9141–9145
17. Zhu M, Huang Y, Huang Y, Li H, Wang Z, Pei Z, Xue Q, Geng H, Zhi C (2017) A highly durable, transferable, and substrate-versatile high-performance all-polymer micro-supercapacitor with plug-and-play function. Adv Mater 29:1605137
18. Lei Z, Chen B, Koo YM, MacFarlane DR (2017) Introduction: ionic liquids. Chem Rev 117:6633–6635
19. MacFarlane DR, Forsyth M, Howlett PC, Pringle JM, Sun JZ, Annat G, Neil W, Izgorodina EI (2007) Ionic liquids in electrochemical devices and processes: managing interfacial electrochemistry. Acc Chem Res 40:1165–1173
20. Qian WJ, Texter J, Yan F (2017) Frontiers in poly(ionic liquid)s: syntheses and applications. Chem Soc Rev 46:1124–1159
21. Dong T, Zhang SJ, Zhang L, Chen SM, Lu XM (2015) Improving cycling performance of $LiMn_2O_4$ battery by adding an ester-functionalized ionic liquid to electrolyte. Aust J Chem 68:1911–1917
22. Pont AL, Marcilla R, Meatza DI, Grande H, Mecerreyes D (2009) Pyrrolidinium-based polymeric ionic liquids as mechanically and electrochemically stable polymer electrolytes. J Power Sources 188:558–563
23. Balducci A, Jeong SS, Kim GT, Passerini S, Winter M, Schmuck M, Appetecchi GB, Marcilla R, Mecerreyes D, Barsukov V, Cantero I, Meatza D, Holzapfel M, Tran N (2011) Development of safe, green and high performance ionic liquids-based batteries (ILLIBATT project). J Power Sources 196:9719–9730
24. Huang KC, Li HH, Fan HH, Guo JZ, Xing YM, Wu XL, Zhang JP (2017) An in-situ-fabricated composite polymer electrolyte containing large-anion lithium salt for all-solid-state $LiFePO_4$/Li batteries. ChemElectroChem 4:1–8
25. Wu X-L, Li Y-H, Wu N, Xin S, Kim J-H, Yan Y, Lee JS, Guo YG (2013) Enhanced working temperature of PEO-based polymer electrolyte via porous PTFE film as an efficient heat resister. Solid State Ionics 245:1–7
26. Appetecchi GB, Kim GT, Montanino M, Carewska M, Marcilla R, Mecerreyes D, De Meatza I (2010) Ternary polymer electrolytes containing pyrrolidinium-based polymeric ionic liquids for lithium batteries. J Power Sources 195:3668–3675
27. Li MT, Yang L, Fang SH, Dong SM, Hirano SI, Tachibana K (2012) Polymerized ionic liquids with guanidinium cations as host for gel polymer electrolytes in lithium metal batteries. Polym Int 61:259–264
28. Li MT, Yang L, Fang SH, Dong SM, Hirano SI, Tachibana K (2011) Polymer electrolytes containing guanidinium-based polymeric ionic liquids for rechargeable lithium batteries. J Power Sources 196:8662–8668
29. Li MT, Yang BL, Wang L, Zhang Y, Zhang Z, Fang SH, Zhang ZX (2013) New polymerized ionic liquid (PIL) gel electrolyte membranes based on tetraalkylammonium cations for lithium ion batteries. J Membr Sci 447:222–227
30. Li MT, Wang L, Yang BL, Du TT, Zhang Y (2014) Facile preparation of polymer electrolytes based on the polymerized ionic liquid poly ((4-vinylbenzyl) trimethylammonium bis(trifluoromethanesulfonylimide)) for lithium secondary batteries. Electrochim Acta 23:296–302

31. Yin K, Zhang ZX, Yang L, Hirano SI (2014) An imidazolium-based polymerized ionic liquid via novel synthetic strategy as polymer electrolytes for lithium ion batteries. J Power Sources 258:150–154
32. Yin K, Zhang ZX, Li XW, Yang L, Tachibana K, Hirano SI (2015) Polymer electrolytes based on dicationic polymeric ionic liquids: application in lithium metal batteries. J Mater Chem A 3:170–178
33. Porcarelli L, Shaplov AS, Salsamendi M, Nair JR, Vygodskii YS, Mecerreyes D, Grbaldi C (2016) Single-ion block copoly(ionic liquid)s as electrolytes for all-solid state lithium batteries. ACS Appl Mater Interfaces 8:10350–10359
34. Tiruye GA, Munoz-Torrero D, Palma J, Anderson M, Marcilla R (2015) All-solid state supercapacitors operating at 3.5 V by using ionic liquid based polymer electrolytes. J Power Sources 279:472–480
35. Du CH, Ma XM, Wu CJ, Cai MQ, Hu MX, Wang T (2015) Polymerizable ionic liquid copolymer P(MMA-co-BVIm-Br) and its effect on the surface wettability of PVDF blend membranes. Chin J Polym Sci 33:857–868
36. Pekel N, Şahiner N, Güven O, Rzaev ZMO (2001) Synthesis and characterization of N-vinylimidazole–ethyl methacrylate copolymers and determination of monomer reactivity ratios. Eurpolym J 37:2443–2451
37. Kumar R, Sekhon SS (2008) Effect of molecular weight of PMMA on the conductivity and viscosity behavior of polymer gel electrolytes containing $NH_4CF_3SO_3$. Ionics 14:509–514
38. Arunkumar R, Babu RS, Usha Rani M, Kalainathan S (2017) Effect of PBMA on PVC-based polymer blend electrolytes. J Appl Polym Sci 134:44939
39. Pandey GP, Hashmi SA (2013) Performance of solid-state supercapacitors with ionic liquid 1-ethyl-3-methylimidazolium tris(pentafluoroethyl)trifluorophosphate based gel polymer electrolyte and modified MWCNT electrodes. Electrochim Acta 105:333–341
40. Liu YQ, Weng B, Razal JM, Xu Q, Zhao C, Hou YY, Seyedin SY, Jalili R, Wallace GG, Chen J (2015) High-performance flexible all-solid-state supercapacitor from large free-standing graphene-PEDOT/PSS films. Sci Rep 5:17045
41. Liew CW, Ramesh S, Arof AK (2015) Characterization of ionic liquid added poly (vinyl alcohol)-based proton conducting polymer electrolytes and electrochemical studies on the supercapacitors. Int J Hydrog Energy 40:852–862
42. Zhang X, Liu T, Zhang SF, Huang X, Xu BQ, Lin YH, Xu B, Li LL, Nan CW, Shen Y (2017) Synergistic coupling between $Li_{6.75}La_3Zr_{1.75}Ta_{0.25}O_{12}$ and poly (vinylidene fluoride) induces high ionic conductivity, mechanical strength, and thermal stability of solid composite electrolytes. J Am Chem Soc 139:13779–13785
43. Liang B, Tang SQ, Jiang QB, Chen CS, Chen X, Li SL, Yan XC (2015) Preparation and characterization of PEO-PMMA polymer composite electrolytes doped with nano-Al_2O_3. Electrochim Acta 169:334–341
44. Yang CY, Sun MQ, Wang X, Wang GC (2015) A novel flexible supercapacitor based on cross-linked PVDF-HFP porous organogel electrolyte and carbon nanotube paper@ π-conjugated polymer film electrodes. ACS Sustain Chem Eng 3:2067–2076
45. Yadav N, Mishra K, Hashmi S (2017) Optimization of porous polymer electrolyte for quasi-solid-state electrical double layer supercapacitor. Electrochim Acta 235:570–582
46. Zhao K, Qin QQ, Wang HF, Yang Y, Yan J, Jiang XM (2017) Antibacterial triboelectric membrane-based highly-efficient self-charging supercapacitors. Nano Energy 36:30–37
47. Kim TY, Lee HW, Stoller M, Dreyer DR, Bielawski CW, Ruoff RS, Suh KS (2010) High-performance supercapacitors based on poly (ionic liquid)-modified graphene electrodes. ACS Nano 5:436–442
48. Zhong XW, Tang J, Cao LJ, Kong WG, Sun Z, Cheng H, Lu ZG, Pan H, Xu BM (2017) Cross-linking of polymer and ionic liquid as high-performance gel electrolyte for flexible solid-state supercapacitors. Electrochim Acta 244:112–118
49. Vijayakumar V, Anothumakkool B, Torris ATA, Nair SB, Badiger MV, Kurungot S (2017) An all-solid-state-supercapacitor possessing a non-aqueous gel polymer electrolyte prepared using a UV-assisted in situ polymerization strategy. J Mater Chem A 5:8461–8476
50. Li ZF, Ma GQ, Ge R, Qin F, Dong XY, Meng W, Liu TF, Tong JH, Jiang FY, Zhou YF, Li K, Min X, Huo KF, Zhou YH (2016) Free-standing conducting polymer films for high-performance energy devices. Angew Chem Int Ed 55:979–982